

# Modelling feeding, growth, and habitat selection in larval Atlantic cod (*Gadus morhua*): observations and model predictions in a macrocosm environment

Trond Kristiansen, Øyvind Fiksen, and Arild Folkvord

**Abstract:** Individual-based models (IBMs) integrate behavioural, physiological, and developmental features and differences among individuals. Building on previous process-based models, we developed an IBM of larval Atlantic cod (*Gadus morhua*) that included foraging, size-, temperature-, and food-limited growth, and environmental factors such as prey-field, turbulence, and light. Direct comparison between larval fish IBMs and experimental studies is lacking. Using data from a macrocosm study on growth and feeding of larval cod, we forced the model with observed temperature and prey-field and compared model predictions with observed distribution, diet, size-at-age, and specific growth rates. We explored implications of habitat selection rules on predicted growth rates. We analyze the sensitivity of model predictions by the Latin Hypercube Sampling method and individual parameter perturbation. Food limitation prevented larvae from growing at their physiological maximum, especially in the period 5–17 days post hatch (DPH). Active habitat selection had the potential to enhance larval growth rates. The model predicted temperature-limited growth rates for first-feeding larvae (5–20 DPH) when prey density is  $>5$  nauplii·L<sup>-1</sup>. After age 20 DPH, maximum modelled growth required a diet of copepodites. Simulated growth rates were close to observed values except for the period just after the start of exogenous feeding when prey density was low.

**Résumé :** Les modèles centrés sur l'individu (IBMs) intègrent les caractéristiques du comportement, de la physiologie et du développement, ainsi que les différences entre les individus. Nous servant de modèles antérieurs basés sur les processus, nous bâtissons un IBM pour les larves de morue franche (*Gadus morhua*) qui inclut la recherche de nourriture, la croissance limitée par la température et l'alimentation, de même que des facteurs du milieu, tels que l'univers des proies, la turbulence et la lumière. Il n'existe pas de comparaisons directes entre les IBM de larves de poissons et les études expérimentales. À l'aide de données provenant d'une étude de la croissance et de l'alimentation de larves de morue en macrocosme, nous avons forcé le modèle avec les températures et les communautés de proies observées; nous avons ensuite comparé les prédictions du modèle à la répartition, au régime alimentaire, à la taille en fonction de l'âge et aux taux spécifiques de croissance observés. Nous avons exploré les conséquences des règles de sélection de l'habitat sur les taux de croissance prédits. Nous analysons la sensibilité des prédictions du modèle par la méthode d'échantillonnage par hypercubes latins et par la perturbation des paramètres individuels. La pénurie de nourriture empêche les larves de croître à leur taux physiologique maximal, particulièrement dans la période des jours 5–17 après l'éclosion (DPH). Une sélection active de l'habitat peut potentiellement améliorer les taux de croissance des larves. Le modèle prédit des taux de croissance limités par la température chez les larves qui se nourrissent pour la première fois (5–20 DPH), lorsque la densité des proies est  $>5$  nauplius·L<sup>-1</sup>. À l'âge de 20 DPH, la croissance maximale prédite par le modèle exige un régime composé de copépodites. Les taux de croissance simulés se rapprochent des valeurs observées à l'exception de la période qui suit immédiatement le début de l'alimentation exogène à un moment où la densité des proies est basse.

[Traduit par la Rédaction]

## Introduction

Individual-based models (IBMs) are an important tool that can integrate from individual-level properties of environmental exposure, behaviour, and physiology to population-

level characteristics of larval fish growth, survival, and spatial distribution (Grimm and Railsback 2005). Presently, there are many attempts to develop coupled biophysical models where IBMs of larval fish are embedded in general circulation models (Werner et al. 2001; Hinrichsen et al.

Received 24 March 2006. Accepted 9 October 2006. Published on the NRC Research Press Web site at <http://cjfas.nrc.ca> on 30 January 2007.  
J19240

T. Kristiansen,<sup>1</sup> Ø. Fiksen, and A. Folkvord. Department of Biology, University of Bergen, P.O. Box 7800, N-5020 Bergen, Norway.

<sup>1</sup>Corresponding author (e-mail: [trond.kristiansen@bio.uib.no](mailto:trond.kristiansen@bio.uib.no)).

**Fig. 1.** (a) Temperature distribution (°C) and (b) average prey abundance (µg·L<sup>-1</sup>) during the macrocosm experiment and observed (c) day and (d) night distribution (%·m<sup>-1</sup>) of larval Atlantic cod (*Gadus morhua*).

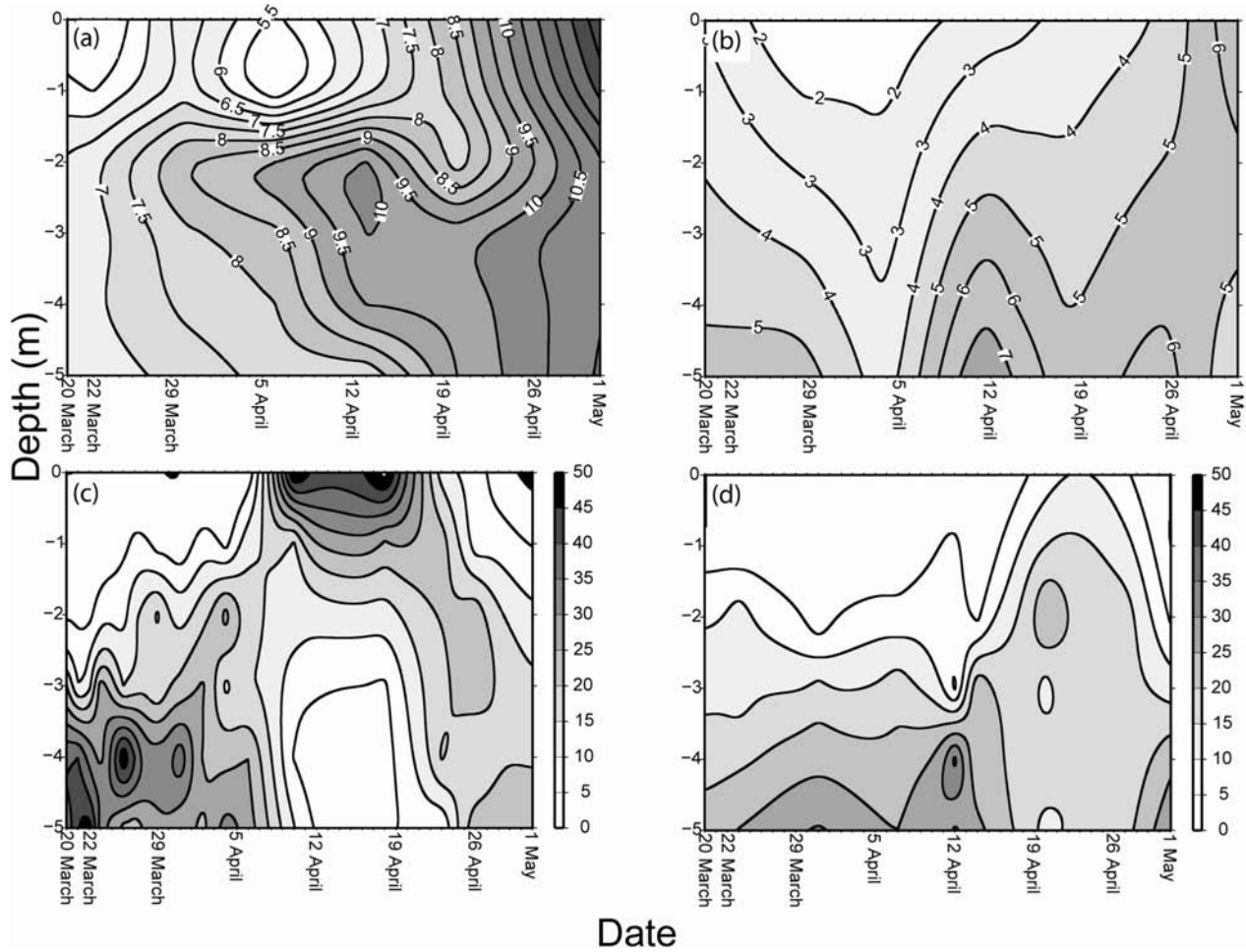


**Table 1.** Length ( $lp_i$ ), width ( $dp_i$ ), and dry weight ( $wp_i$ ) for the 13 various zooplankton categories ( $i$ ) available as prey in the pond.

	R	NI	NII	NIII	NIV	NV	NVI	CI	CII	CIII	CIV	H	M
$lp_i$ (mm)	0.10	0.22	0.27	0.40	0.48	0.55	0.61	0.79	1.08	1.38	1.80	0.30	0.60
$dp_i$ (mm)	0.10	0.10	0.10	0.10	0.15	0.18	0.20	0.22	0.25	0.31	0.40	0.10	0.30
$wp_i$ (µg)	0.16	0.33	0.49	1.0	1.51	2.09	2.76	4.18	13.24	23.13	63.64	0.30	1.00

**Note:** R, rotifer; N, nauplius; C, copepodite; H, harpactacid; M, miscellaneous. Sizes taken from Lough et al. (2005). Image area of prey ( $A_p$ , mm<sup>2</sup>) is estimated as  $lp \times dp \times 0.75$  (elongate prey).

2002; Lough et al. 2005). However, direct comparisons between model predictions and the observed growth patterns or feeding habits of larvae in natural or seminatural environments are rare. Therefore, direct comparisons between model predictions and observations of larval fish feeding, growth, and spatial distribution are warranted. Such efforts may strengthen our confidence in predictions from large-scale, physical-biological-coupled models. Controlled environments in macrocosms or landlocked fjords provide a balance between the realism of a natural habitat and the tractability of the laboratory (Folkvord et al. 1994). Information on the environmental conditions and larval properties from such studies can be used as forcing data to drive IBMs.

In the pelagic realm, vertical environmental gradients are typically much stronger than horizontal gradients. Therefore,

when implementing IBMs into circulation models, accurate representation of the vertical distribution is important for predicting the exposure of larvae to environmental factors. Also, the horizontal dispersal of larvae often depends on their vertical positioning (Vikebø et al. 2005). However, little information exists on criteria for habitat selection of larval Atlantic cod (*Gadus morhua*). This is particularly so for larvae facing trade-offs between food availability, temperature, advection, and predation risk. Here, we present a mechanistic model of foraging and growth of cod larvae. The feeding processes are adopted from Fiksen and MacKenzie (2002), while our formulation of assimilation and transformation of energy from prey to larval tissue and growth is new. It incorporates the empirical models developed by Finn et al. (2002) and Folkvord (2005). Explicit

simulations of the macrocosm experiment by Folkvord et al. (1994) allow for direct comparison between model predictions and observed properties of the larvae in a monitored, nearly predator-free environment. We compare modelled and observed growth and diet of larvae for the first 42 days of their life. In addition, we explore the effects of habitat selection by the larvae on realized growth rates in the pond.

### Biological background: the macrocosm experiment

This model effort uses observed temperature and prey density from a macrocosm experiment (Folkvord et al. 1994) as forcing. Observations of larval growth and weight at dates are compared with model predictions. Below, we provide a brief summary of the Folkvord et al. (1994) experiment.

#### Sampling

In spring 1983, larval Atlantic cod were released in five cohorts separated by 10-day intervals into the 5.5 m deep naturally enclosed 63 000 m<sup>3</sup> Hyltrollen (Folkvord et al. 1994). Fish larvae were 5 days post hatch (DPH) at the day of release and still at the yolk-sac stage. A total of 40 000 larvae samples were collected between 20 March and 3 May 1983, and 4354 larvae were individually measured. The environment was monitored by weekly measurements of temperature (Fig. 1a) and zooplankton biomass (Fig. 1b) at 1 m intervals from the surface to the bottom (Folkvord et al. 1994). Observations of zooplankton and temperature are available to day 42 (47 DPH) of the experiment.

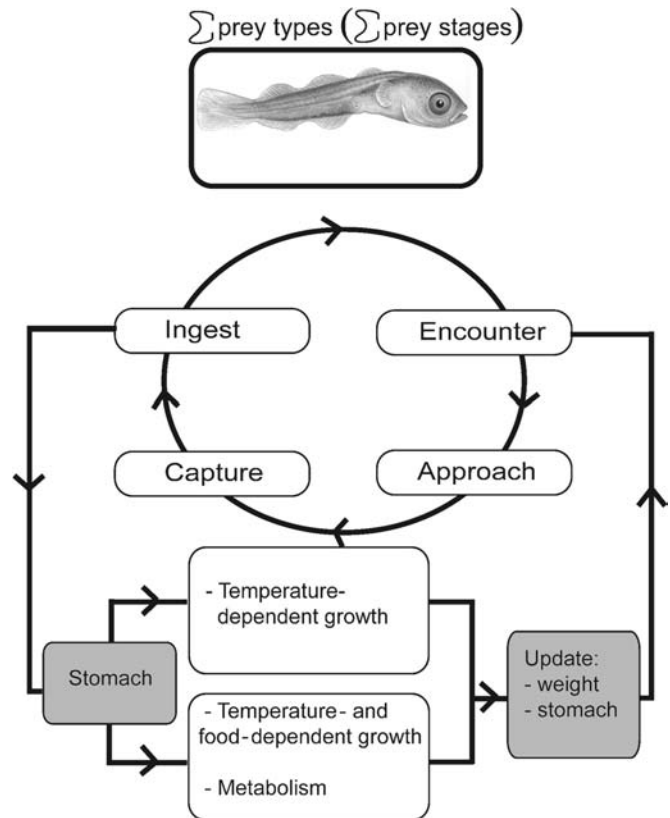
#### The environment

An average turbulent dissipation rate was estimated using the mean wind field obtained from the Meteorological Institute in Norway for a nearby station (Flesland) and the empirical relationship between wind and turbulence from Mackenzie and Leggett (1993). Both temperature and zooplankton concentrations showed strong vertical and temporal variation (Fig. 1). Initially, strong vertical gradients characterized the hydrography after a cold weather period with patches of ice at the surface. By mid-April, most of the gradients had eroded and the water column was mixed (Fig. 1a).

#### Prey

In late March, total zooplankton biomass was very low at the surface but increased towards the bottom (Fig. 1). As time passed, the zooplankton became distributed homogeneously in the water column. Prey types available in the pond were nauplii and copepodite stages of *Calanus finmarchicus*, rotifers, and harpacticoids. Rotifers were an important prey item for first-feeding larvae (Folkvord et al. 1994). A peak in abundance of rotifers occurred in the beginning of April (33·L<sup>-1</sup> at the surface). Total prey density rarely exceeded 10·L<sup>-1</sup> with an average close to 6·L<sup>-1</sup> (Folkvord et al. 1994). Mean, standard deviation, minimum, and maximum values for the period 20 March – 1 May were 1.0 ± 5.0·L<sup>-1</sup> (0.0–33·L<sup>-1</sup>) for rotifers, 2.1 ± 1.7·L<sup>-1</sup> (0.1–8.3·L<sup>-1</sup>) for nauplii, 0.6 ± 0.4·L<sup>-1</sup> (0.1–1.9·L<sup>-1</sup>) for copepodites, 0.5 ±

Fig. 2. Flow chart of the individual-based model (IBM) where submodels are open boxes and state variables are shaded boxes. Each hourly calculations start with estimation of encounter, approach, capture, and ingestion for 13 prey types and sizes. Ingested biomass is stored in the stomach variable and determines together with ambient temperature the corresponding growth. The model has a spatial and temporal resolution of 1 m. Larval drawing by Tamara L. Clark, Woods Hole, Massachusetts.



1.0·L<sup>-1</sup> (0.0 ± 5.8·L<sup>-1</sup>) for harpacticoids, and 1.7 ± 2.2·L<sup>-1</sup> (0.3 ± 13.6·L<sup>-1</sup>) for miscellaneous species.

The sampling only separated between nauplii and copepodites. To obtain smaller incremental steps between size-classes of prey, we divided the *C. finmarchicus* data into developmental stages NI–NVI for nauplii and CI–CIV for copepods (Table 1). We assumed an exponential decrease in numbers between stages, where prey concentrations and prey size spectra correspond to estimated densities of nauplii and copepodites (Table 1).

### Model description

The model description follows the outline recommended by Grimm and Railsback (2005) (PSPC + 3).

#### Purpose

This IBM simulates the early life history of larval cod based on environmental factors and underlying processes that we believe are important. Each process is formulated and parameterized from laboratory experiments conducted on larval cod (Fiksen and MacKenzie 2002). The combination of these processes describes mechanistically how larval

**Table 2.** Variables and parameters from the IBM.

Symbol	Description	Units	Value
$SGR^a$	Specific growth rate	%·day <sup>-1</sup>	Eq. 2
$R^b$	Respiration rate	μg	Eq. 1
$s$	Stomach size	μg·μg <sup>-1</sup> ·individual <sup>-1</sup>	Eq. 5
$wp_i$	Weight of prey of type $i$	μg	Table 1
$lp_i$	Length of prey type $i$	mm	Table 1
$dp_i$	Width of prey type $i$	mm	Table 1
$e^c$	Encounter rate	Prey·s <sup>-1</sup>	$e = \frac{2}{3} \pi f r^3 + \pi r^2 N f \lambda \sqrt{u^2 + 2\omega^2}$
$f^c$	Pause frequency	s <sup>-1</sup>	0.43
$N$	Prey density	mm <sup>3</sup>	
$r^d$	Distance of perception	mm	$r^2 \exp(cr) = E' CA_p \frac{E_b}{E_b + K_e}$
$u$	Prey swimming speed	mm·s <sup>-1</sup>	$100 \times lp_i$
$\omega^e$	Turbulent velocity	mm·s <sup>-1</sup>	$\omega = \sqrt{3.615(\varepsilon r)^{0.667}}$
$\lambda^c$	Pause duration	s	2.0
$E'^s$	Eye sensitivity of larva	Dimensionless	$E' = \frac{SL^2}{C \times 0.1 \times 0.2 \times 0.75}$
$C^d$	Prey inherent contrast	Dimensionless	0.4
$A_p^f$	Image of elongate prey	mm <sup>2</sup>	$lp \times dp \times 0.75$
$K_e^d$	Larva half-saturation parameter	μmol·m <sup>-2</sup> ·s <sup>-1</sup>	1.0
$E_b^d$	Light	μmol·m <sup>-2</sup> ·s <sup>-1</sup>	$E_b(z, h) = E_0(h) \exp(-zk)$
$A^h$	Assimilation efficiency	Dimensionless	0.75
$c$	Beam attenuation coefficient	m <sup>-1</sup>	$3k$
$\varepsilon^e$	Turbulent dissipation rate	kg·m <sup>-2</sup> ·s <sup>-3</sup>	$\varepsilon = 5.82 \times 10^{-9} W^3$
$W$	Windspeed	m·s <sup>-1</sup>	3.0
$k$	Attenuation coefficient	m <sup>-1</sup>	0.18

<sup>a</sup>Folkvord (2005).<sup>b</sup>Finn et al. (2002).<sup>c</sup>MacKenzie and Kiørboe (1995).<sup>d</sup>Aksnes and Utne (1997).<sup>e</sup>MacKenzie and Leggett (1993).<sup>f</sup>Fiksen and Folkvord (1999).<sup>g</sup>Fiksen and MacKenzie (2002).<sup>h</sup>Kiørboe (1989).

cod encounter, capture, and ingest food and use the energy for growth. The main purpose is to evaluate model performance in a well-studied seminatural situation.

### Structure

We simulated growth for a period of 5–47 DPH for 160 individual cod larvae in a closed macrocosm with no predators assuming no mortality and no interactions among individual larvae. Behavioural responses to changes in the environment were restricted to vertical movements with a spatial resolution of 1 m and a temporal resolution of 1 h.

### Processes

Submodels govern the interaction between environmental forcing (temperature, turbulence, and zooplankton density) and the dynamic state variables weight, stomach content, and length. These states are updated once every hour (Fig. 2). A key element is the mechanistic foraging submodel combined with a stomach as a state variable. Ingested mass or energy results from the successful comple-

tion of sequential processes: encounter, approach, and capture (Fiksen and MacKenzie 2002). The foraging processes are iterated for all prey types and size categories (Fig. 2). Holling's (1966) disc equation ensures that the total time spent handling prey reduces available search time. Stomach fullness and body mass determine whether growth is only temperature dependent or also food limited.

### Concepts

An important and difficult topic for larval fish modelling is the behavioural positioning of the larvae in environmental gradients. We expect strong selection pressures on habitat selection in larval fish, since the pelagic environment is typically characterized by strong vertical gradients of variables related to growth (temperature, prey concentrations, light, and turbulence), predation risk (distribution and search efficiency of predators), and the probability of being advected out of favourable areas (Werner et al. 1993; Vikebø et al. 2005). Here, we explore the consequences of four different vertical behavioural rules: (i) larvae move along the depth of

**Fig. 3.** Growth rates (left panels) for three fish sizes, (a) 0.1, (b) 1.0, and (c) 100 mg, experiencing a range of ingestion rates (0–0.6 g·g<sup>-1</sup>·day<sup>-1</sup>) and temperatures (4–16 °C). Also shown are larval and juvenile (0.01–100 mg) growth rates assuming three fixed ingestion rates (d) 0.8, (e) 0.3, and (f) 0.0 g·g<sup>-1</sup>·day<sup>-1</sup> for different temperatures (4–16 °C).

observed larval maximum abundances (ObsD), (ii) larvae follow the depth of highest temperature (HighT), (iii) larvae move along the depth with highest prey biomass (HighP), and (iv) larvae find the depth that yields the highest growth rate (HighG). We also included a simulation of larvae without active selection, i.e., larvae that move randomly up or down the water column. Our null hypothesis was that individuals with a strategy would grow faster than individuals moving randomly in the water column. To test this, we recorded average weight-at-age and depth distribution of 100 individuals for 32 days with random vertical positioning. All larvae were initialized with a start weight of 58 µg.

### Initialization

We used observed data on each of four dates (26 and 31 March and 6 and 10 April) to describe the initial population weight distribution. For each date (11, 16, 22, and 26 DPH), we drew 160 (maximum number of larvae sampled at 16 DPH) individual weights randomly from the observations to yield averages of  $58 \pm 9$ ,  $112 \pm 22$ ,  $234 \pm 48$ , and  $410 \pm 87$  µg, respectively. Using the four start dates and 160 individuals, simulations were repeated for the four rules. This resulted in 2560 individual realizations.

The simulation initiated on 10 April was run until 47 DPH and was compared with final observations from the pond on day 49, the final day of the Folkvord et al. (1994) experiment. This provides us with as many direct comparisons between predictions and observations as possible and also allows for identifying under which environmental conditions the model failed.

### Input

Observed (Folkvord et al. 1994) prey density and turbulence were input to the foraging processes and temperature for the growth processes. We modelled light as a function of date, time of day, and latitude.

### Submodels

The IBM was written as an object-oriented Fortran 90 code, which allows for tracking properties for every individual. Following is a detailed description of the various submodels.

#### Larval feeding processes

Prey encounter rate, pursuit success, and capture success determine larval feeding success. We applied the detailed and mechanistic model by Fiksen and MacKenzie (2002) based on earlier developments (MacKenzie and Kjørboe 1995; Aksnes and Utne 1997; Caparroy et al. 2000). This model predicts (i) prey encounter rates as a function of prey characteristics, larval size, ambient light, turbulence, and prey density and the probability that (ii) prey detect the approaching larvae and escape (Psa), (iii) prey are advected out of the larva's perception range owing to turbulence (Psp), and (iv) prey are successfully captured and ingested (Pca).

Prey ingestion is limited by stomach capacity, while the prey items that compose the diet are estimated from all prey items captured within the last time step. Predictions from this model generated larval prey size selectivity in agreement with observations by Munk (1997). Key variables and parameter values are defined in Table 2. Visual foragers depend on light. Light conditions  $E_b$  vary with time of day  $h$  and depth  $z$  and are a function of the surface light  $E_0$  and the diffuse light attenuation  $k$  (Table 2). Surface light is calculated according to time of day, latitude (60°N), and day of the year (here, 20 March – 2 May 1983).

#### Respiration rates

Routine respiration rate of larval cod was thoroughly estimated by Finn et al. (2002). Routine respiration  $R$  (µg·individual<sup>-1</sup>·h<sup>-1</sup>) varies with dry-weight body mass  $w$  (mg) and temperature  $T$  (°C) as

$$(1) \quad R = 2.38 \times 10^{-7} w^{0.9} \exp(0.088T)$$

Respiration rates were measured in light and darkness (Finn et al. 2002). Higher values occurred in light than in darkness, indicating that the values from darkness were closer to resting respiration. In the present model, we have applied the averaged value for  $R$ . The metabolism is elevated by a factor of 2.0 (Lough et al. 2005) when light conditions are suitable for foraging (visual range  $\geq 1.0$  mm) and the larvae are active.

#### Size- and temperature-limited growth rate

If the larvae ingest more food than they can process and assimilate, then size- and temperature-dependent physiological processes will limit their growth. We applied the model derived from extensive laboratory rearing experiments on coastal cod by Otterlei et al. (1999) and Folkvord (2005) to find larval specific growth rates (SGR, %·day<sup>-1</sup>) under such conditions:

$$(2) \quad \text{SGR}(w, T) = a - b \ln(w) - c \ln(w)^2 + d \ln(w)^3$$

where SGR is the specific growth rate in percentage per day, expressed as a function of temperature ( $T$ ) and dry mass ( $w$ , mg), and  $a = 1.08 + 1.79T$ ,  $b = 0.074T$ ,  $c = 0.0965T$ , and  $d = 0.0112T$  (Folkvord 2005). The SGR can be expressed as specific growth rate  $g$  per time step ( $dt$ , day<sup>-1</sup>),  $g = \ln[(\text{SGR}/100) + 1]/dt$ .

#### Larval state variables and food-limited growth

Larvae are characterized by the state variables body mass ( $w$ , dry weight) and stomach fullness ( $s$ ). The maximum energy content of the stomach ( $s$ ) is set to 6.0% of the total weight, which corresponds to observations of stomach content and size of cod larvae on Georges Bank (E. Broughton, National Marine Fisheries Service, NOAA, Northeast Fisheries Science Center, Woods Hole, MA 02543, USA, personal communication) and to the upper limit of ingested material used by Lough et al. (2005). The amount of food in the stomach and the growth potential of the larvae determine

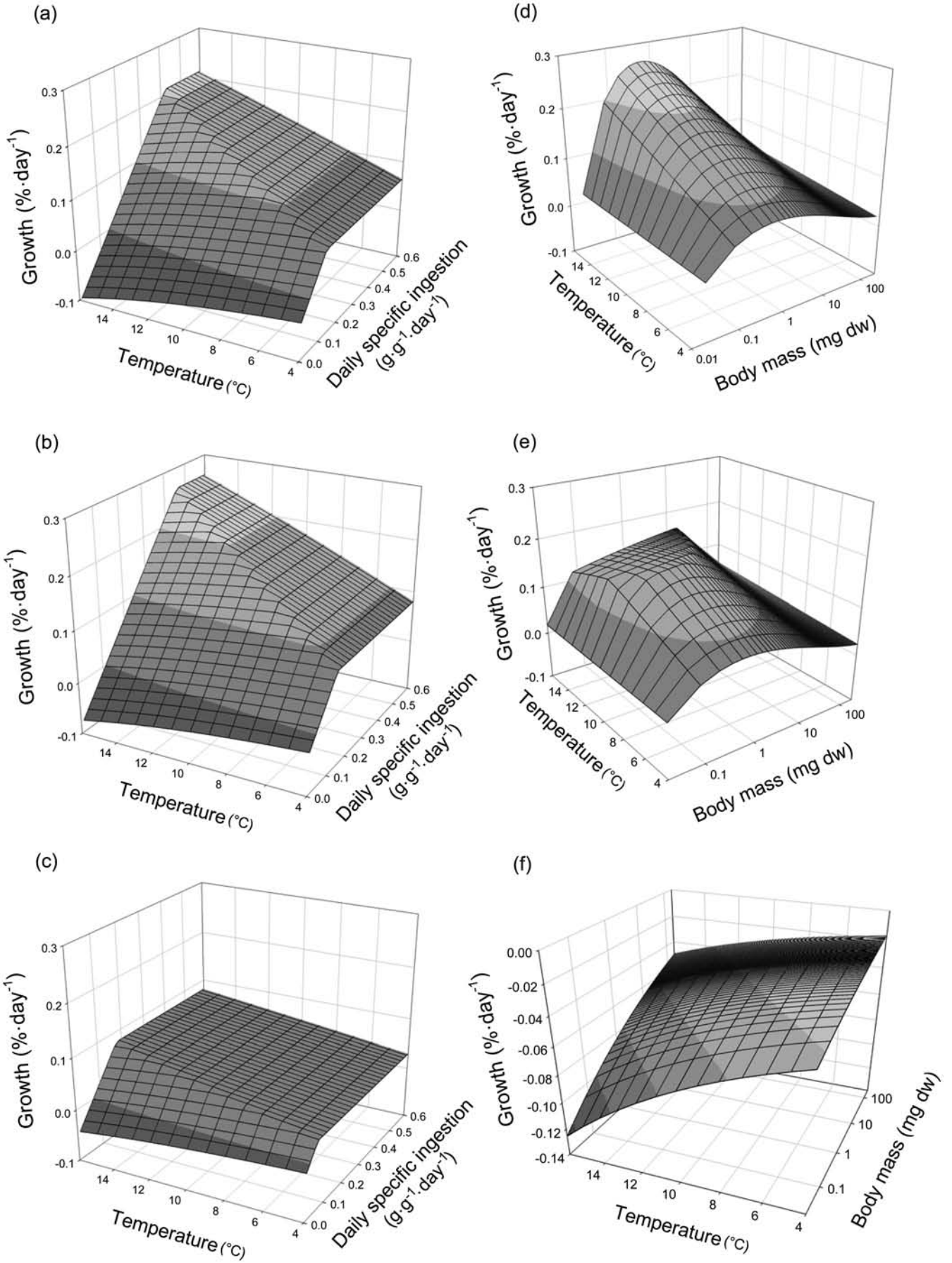


**Table 3.** Variables and parameters examined in the sensitivity analysis, divided into internal and external variables, and further grouped into submodel level.

Parameter-variable	Mean value (min.–max.)	$r^2$			10% increase individual parameter perturbation (% increase in weight from base after 48 h)	
		5 mm	11 mm	Submodel	5 mm	11 mm
<b>External</b>						
Temperature (°C)	7.0 (6.5–7.5)	0.05	0.98	Environment	0.4	1.6
Prey density (L <sup>-1</sup> )	2.5 (0.5–4.5)	0.88	0.02		0.4	0.05
Surface wind	3.0 (1.0–5.0)	0.00	0.00		0.1	0.01
Surface light (μmol·m <sup>-2</sup> ·s <sup>-1</sup> )	250 (200–300)	0.00	0.00		0.0	0.0
Beam attenuation coefficient (m <sup>-1</sup> )	0.18 (0.1–0.3)	0.00	0.00		-0.3	0.0
Attenuation coefficient (m <sup>-1</sup> )	0.54 (0.33–0.89)	0.00	0.00		-0.1	0.0
Sum		0.94	1.00			
<b>Internal</b>						
Initial perception (mm <sup>2</sup> )	0.015 (0.014–0.016)	0.00	0.01	Mechanistic foraging	-0.5	-0.06
Attack speed (m·s <sup>-1</sup> )	10 (8–12)	0.34	0.08		2.9	0.02
Escape speed (m·s <sup>-1</sup> )	100 (80–120)	0.32	0.08		-0.1	-0.07
Mean jump angle (rad)	π/6 (0.3–0.7)	0.12	0.01		-0.3	0.0
Half-saturation parameter	1.0 (0.001–5)	0.00	0.00		-0.2	0.0
Activity (dimensionless)	2.0 (1.5–2.5)	0.00	0.00	Bioenergetic	1.4	0.0
Respiration exponent (dimensionless)	0.9 (0.85–0.95)	0.00	0.01		1.4	0.0
Gut size (% dry weight)	0.06 (0.05–0.07)	0.03	0.24		0.45	0.5
Assimilation (dimensionless)	0.75 (0.6–0.9)	0.00	0.01		3.1	0.0
Sum		0.81	0.45			

**Note:** Mean values of the parameter distribution are shown together with the range (min.–max.). The influence ( $r^2$ ) from each parameter on the simulated weight (after 48 h) is given for two larval sizes (5 and 11 mm). By increasing the parameter value by 10%, the corresponding increase in weight (% increase from base run) is given in the individual parameter perturbation columns for two sizes of larval cod.

whether growth is maximal (size and temperature limited) or food limited.

The mass (or energy)  $D$  required to sustain maximal growth within each time step is given by

$$(3) \quad D = dt(gw + R)/A$$

Here,  $A$  is the assimilation efficiency equal to 0.75, correcting for energy losses through feces and specific dynamic action (Kjørboe 1989). The stomach then acts as a reactor and dynamic storage where mass is withdrawn depending on potential growth. The stomach fullness is a function of previous state  $s_t$ , digested material  $D$ , and ingestion  $i$ :

$$(4) \quad s_{t+1} = s_t - D + i$$

The change in body mass  $dw$  within each time-step is then given by

$$(5) \quad \frac{dw}{dt} = \begin{cases} gw & \text{if } D \leq s_t \\ sA - R & \text{if } D > s_t \end{cases}$$

This is where growth becomes either food or temperature limited. If stomach content  $s_t$  can supply the matter and energy required  $D$  ( $D = s_t$ ), then growth proceeds at maximum rate. Otherwise, if  $D > s_t$ , then what is in the stomach is processed and turned into body mass. The predicted growth rates of larval cod under various temperatures, body mass, and prey ingestion rates are presented in Fig. 3. This ap-

proach integrates solid laboratory studies on larval cod growth and metabolism and a simple, but reasonable, representation of mass and energy flow through the larvae. The model predicts that growth drops linearly with food availability below a threshold that depends on both temperature and larval weight (Fig. 3c). It captures the general view that food requirements are higher when growth rates are high and acts as an interpolation between the food-satiated growth pattern observed by Folkvord (2005) and the starving case of Finn et al. (2002) (Fig. 3b).

## Sensitivity analysis

Trust in model predictions is gained through validation and testing of the IBM. Comparison between simulation results and observations may increase confidence in the hypotheses formalized in the model, depending on its ability to match observed patterns. Also, the importance of submodels in a complex model can be analyzed through sensitivity analyses. If small changes in parameter values generate large responses, the model is sensitive to the parameter.

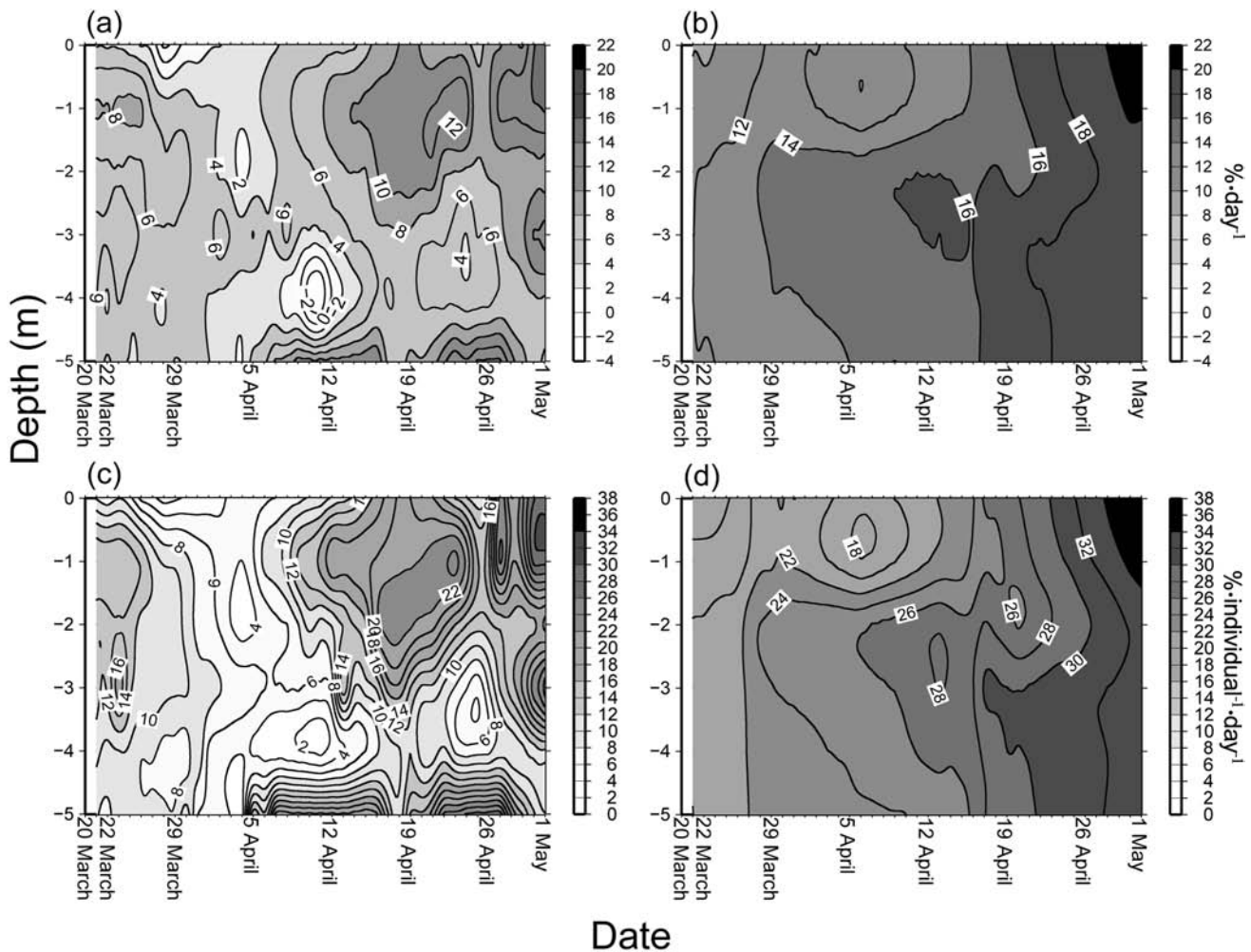
Sensitivity analysis of the IBM was performed using a Monte Carlo simulation where parameter values are randomly selected from a distribution. We implemented this method using Latin Hypercube Sampling (Rose 1987; Rose et al. 1991b) and used it to determine the contribution of parameter variation to prediction error (Bartell et al. 1986). First, we assigned a specific distribution for all parameters

**Table 4.** Density of *Calanus finmarchicus* (nauplii and copepodites) in the water column as experienced by a larva according to vertical behavioural rule and age.

Simulation period (DPH)		Mean density (no.·L <sup>-1</sup> ± SD (min.–max.))			
		ObsD	HighT	HighP	HighG
5–22	Total prey density	2.4±0.8 (1.0–4.0)	2.7±0.9 (0.9–4.4)	4.8±2.2 (1.2–10.0)	3.5±2.0 (0.9–10.0)
	Available for larva	1.2±0.6 (1.3–2.9)	1.3±0.5 (0.4–2.6)	2.8±1.7 (0.4–6)	1.9±1.2 (0.7–5.7)
22–47	Total prey density	2.4±0.7 (1.4–4.0)	2.7±1.0 (0.9–4.4)	6.1±1.8 (4.0–10.0)	2.7±0.9 (0.9–4.3)
	Available for larva	2.1±0.7 (1.0–3.7)	2.1±0.8 (0.9–3.8)	5.4±1.6 (3.3–9.0)	2.1±0.8 (0.9–3.8)

**Note:** The simulation period for the first 17 days post hatch (DPH) and that for the last 25 DPH are separated, as the size of the larvae in the time windows differs significantly and thereby the number of available prey types for ingestion. Only *C. finmarchicus* is considered, as this is the dominant prey item found in gut analysis (Folkvord et al. 1994) both in observations and in simulations. ObsD, depth where maximum abundances of larvae were observed during assessment; HighT, depth of highest temperature; HighP, depth with highest prey biomass; HighG, depth that yields the highest growth rate.

**Fig. 4.** (a and b) Specific growth rates and (c and d) specific ingestion rates for a larva of fixed size, (a and c) 5 and (b and d) 8 mm, experiencing the same environmental and biological conditions. Values are calculated at fixed depths of 1 m resolution.



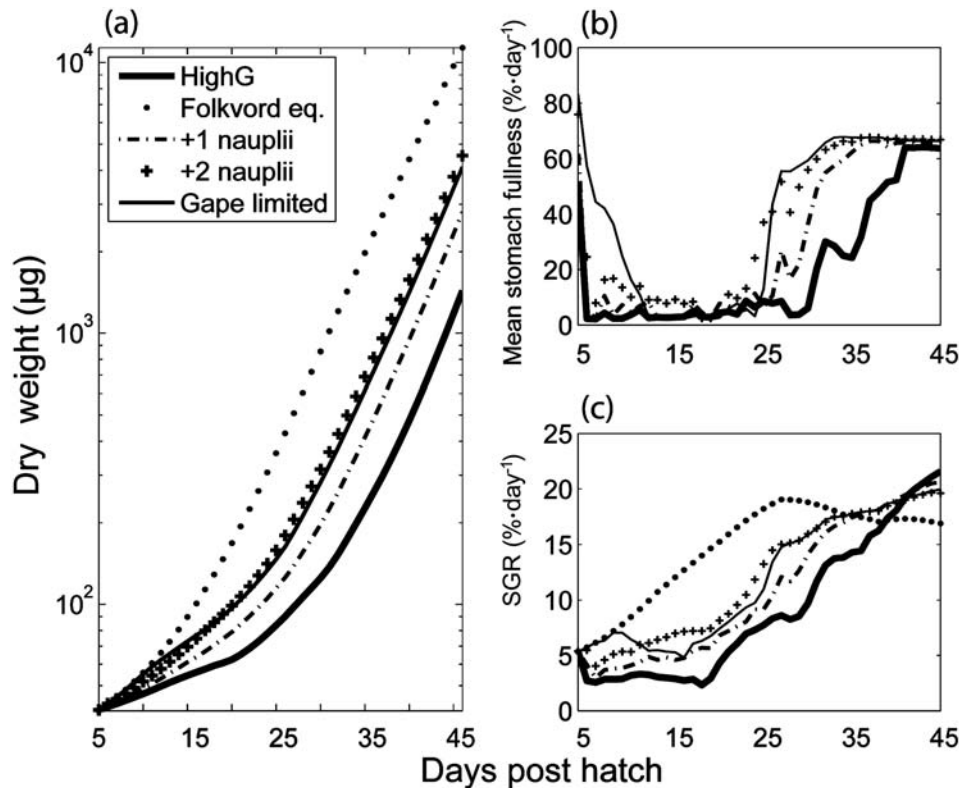
included in the error analysis. The nominal value for each parameter defines the mean value of the distribution. We then drew values randomly from the distributions to create a set of parameter values in each model realization.

A typical approach to sensitivity analysis in IBMs is the individual parameter perturbation method where each variable–parameter in the model is varied ±10% or ±20% between simulations. Model results (weight in this case), with and without this change, determine the impact of the

change in variable value. Although this method leaves us with an indication of the sensitivity of that particular variable, the results can be biased if different processes behave in a nonlinear fashion and interaction exists between variables (Gardner and O’Neill 1981). We included the individual parameter perturbation approach as a companion to the error analysis.

The Monte Carlo error analysis combined with the Latin Hypercube Sampling approach has been used by several au-

**Fig. 5.** Simulated state variables (mean) for 10 larvae ( $35.4 \pm 5.6 \mu\text{g}$ ) over 42 days using vertical positioning rule HighG (depth that yields the highest growth rate). (a) Dry weight, (b) specific growth rate (SGR), and (c) stomach fullness (% of maximum (6% dry weight)) (averaged over 24 h) increase when the prey density in the pond is increased by 1 or 2 nauplii·L<sup>-1</sup>. The potential temperature-dependent (food-unlimited) growth is marked with circles (Folkvord equation). Excluding the mechanistic submodel from the individual-based model (IBM) and assuming that prey is captured if  $l_p/SL < 0.08$  is marked “gape limited”.



thors (Rose et al. 1991a; Letcher et al. 1996; Megrey and Hinckley 2001). In general, these studies found the methods to provide similar results for linear models. We applied the error analysis to the IBM model in two steps by varying (i) six of the external (environmental) variables and (ii) 10 of the internal variables.

We assumed a normal distribution of both internal and external parameters by defining a mean, minimum, and maximum value of each parameter (Table 3). Each parameter distribution was sampled 300 times. During sensitivity analysis of the internal parameters, the environmental variables are not kept constant but vary according to observations. Internal and external parameter analysis resulted in two data sets of size 300 times 11 and 7 (parameters and simulated larval weight), respectively. These data sets were further analysed statistically by simple correlation analysis (Pearson). Correlation between parameters and model results determines the individual contribution from each parameter to model variance. We repeated the analysis for two sizes of larval cod (5 and 11 mm).

## Results

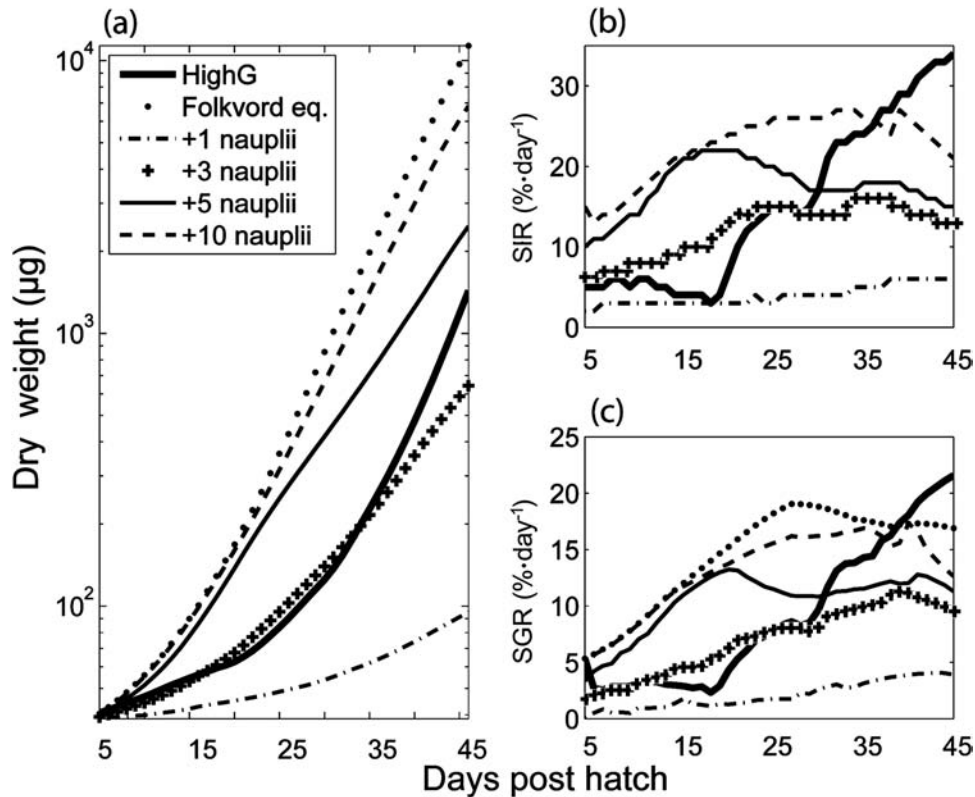
### Sensitivity analysis

The Monte Carlo sensitivity analysis revealed interesting properties of the model. In particular, growth rates were sensitive to variance in certain variables, which differed for

large and small larvae (Table 3). For small larvae (5 mm), prey density strongly influences growth. The range of prey density varied between 0.8 and 10 nauplii·L<sup>-1</sup> depending on choice of vertical rule. Estimated prey concentration within edible size range depended on larval size and vertical rule (Table 4), with very low values for age 5–22 DPH larvae (0.4–6 nauplii·L<sup>-1</sup>). For small larvae, the prey size category available for capture is limited to rotifers and small nauplii (NI–NIII) (Table 1). The sensitivity of the internal parameters revealed that small changes in prey escape speed and larval attack speed can increase or decrease the range of possible prey items (Table 3). In a food-limited situation, this is critical to maintain high growth rates. Larger larvae (11 mm) are unaffected by variation in prey density, as long as the values exceed 2–3 nauplii·L<sup>-1</sup> (Table 4), and variance in growth is explained almost solely by the changes in temperature ( $r^2 = 0.98$ ) (Table 3). This situation also explains why parameters related to foraging efficiency are sensitive for small but not for larger larvae. Similarly, gut size is important for larger larvae, since maintaining growth during night is occasionally dependent on stomach capacity.

Variation in surface light, beam attenuation, and extinction coefficient does not influence the result at all, mainly because light conditions limit foraging only at sunset and at night. The pond is shallow so that light is not the important limiting factor; this has been shown to be so in models of cod in marine environments (Lough et al. 2005).

**Fig. 6.** Simulated state variables (mean) for 10 larvae ( $35.4 \pm 5.6 \mu\text{g}$ ) over 42 days using vertical positioning rule HighG. (a) Dry weight, (b) specific ingestion rate (before assimilation), and (c) specific growth rate increase gradually as prey concentration is raised from 1 to 10 nauplii·L<sup>-1</sup>. The potential temperature-dependent (food-unlimited) growth is marked with circles (Folkvord equation).



Comparison between simulation runs with a 10% increase in parameter values (individual parameter perturbation method) produces low impact on the simulated weight over 48 h. The growth difference was generally lower than 1%, with the exception of the attack speed of the larvae and the prey escape speed for small larvae.

### Vertical behaviour and growth rates

Behavioural conduct in a spatial environment affects the potential growth rates for small larvae, even in a pond of only 5 m depth. Modelled growth and ingestion rates for a 5 mm larva vary considerably between depths (Figs. 4a and 4c). One of the rules applied for habitat selection is related to growth (HighG), and therefore, modelled habitat selection becomes dependent on stomach fullness, temperature, and prey density (Figs. 5 and 6). Larvae adapting to rule HighG achieve the highest growth rates. Larvae of size 5 mm are mechanically restricted to forage on rotifers and copepod nauplii compared with 8 mm larvae that are capable of capturing copepodites. This results in large depth-dependent differences in growth rates for the two sizes of larval cod (Fig. 4) that experience the same habitat. Growth rates are mainly temperature dependent for 8 mm larvae, while growth of a 5 mm larva depends on the correct choice of habitat. Given the relatively low prey concentrations found in the pond (Table 4), a small increase in nauplii (1–2·L<sup>-1</sup>) increases the growth rates considerably for small larvae, especially at the onset of feeding (Fig. 5). The minimum prey density necessary to obtain purely temperature-dependent

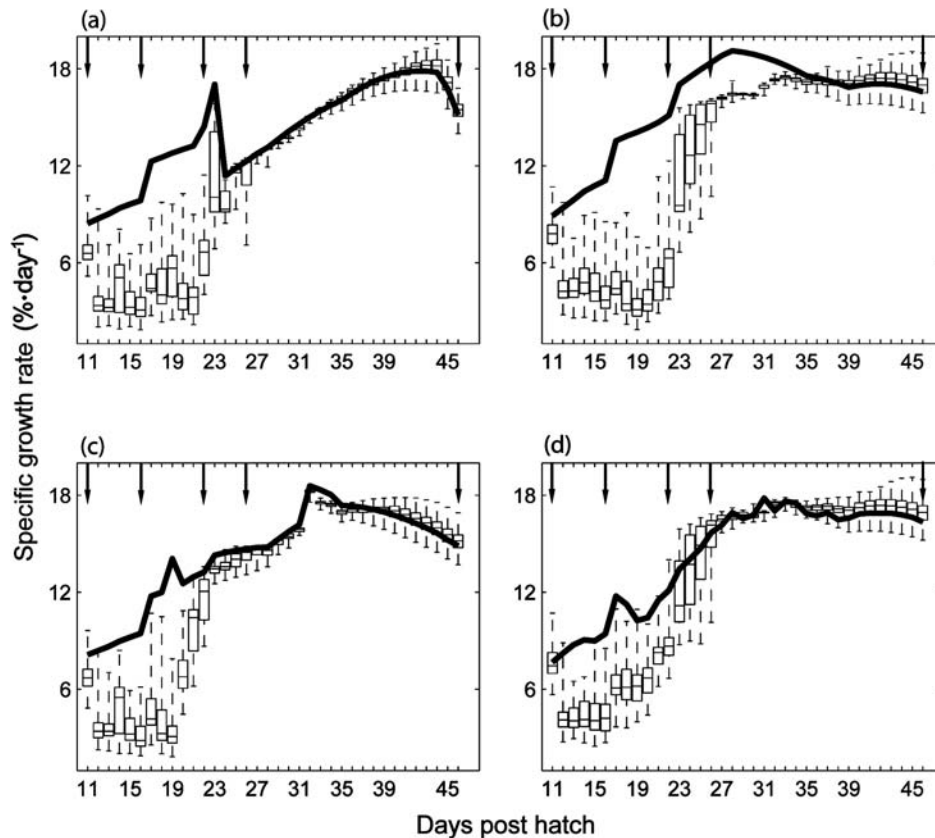
growth rates was analyzed by increasing the prey concentration of nauplii (NI) in the macrocosm from 1 to 10·L<sup>-1</sup> (Fig. 6). A prey density of >10 nauplii·L<sup>-1</sup> enables small larvae (5 mm) to encounter and capture enough prey to sustain the energetic demands of temperature-dependent growth (Fig. 6), although at 25 DPH, growth is food limited, and the larva needs to switch to or include copepodites in the diet to sustain optimal growth rates. Otherwise, the larva is eventually limited by the encounter rate and ceases to capture enough prey. To determine the effect of the mechanistic submodel, we modelled growth where foraging is gape limited and where upper prey length to predator length ratio is a maximum of 8%. Corresponding growth increases equal to an increase in prey density of 2 nauplii·L<sup>-1</sup> (Fig. 5).

Average observed growth rates for the population aged 5–25 DPH were 12.7%·day<sup>-1</sup> (Folkvord et al. 1994), while simulated growth rates depended on the choice of vertical behavioural rule, 9.1%, 10.5%, 10.7%, and 11.2%·day<sup>-1</sup> for ObsD, HighT, HighP, and HighG, respectively (Fig. 7). Simulated growth rates for larval age 5–22 DPH were lower than observed, but the difference diminished after 22 DPH as the simulated larvae increased in size and grew close to observations (Figs. 7 and 8).

### Diet

Gut analysis of larval cod revealed a diet consisting of rotifers and nauplii for the first 20 DPH (Folkvord et al. 1994) and then switched to a diet composed mainly of copepodites (90% of the energy and 20% of the prey items in the stom-

**Fig. 7.** Simulated growth rates for 160 individual larvae. Model runs are initialized with the observed (Folkvord et al. 1994) weight distribution at 11, 16, 22, and 26 days post hatch (DPH) (arrows) using four vertical positioning rules, (a) ObsD (depth where maximum abundances of larvae were observed during assessment), (b) HighT (depth of highest temperature), (c) HighP (depth with highest prey biomass), and (d) HighG (depth that yields the highest growth rate). Temperature-limited growth rate is estimated using the average weight distribution for each day (line) and defines the upper physiological restricted growth rate for the given environment.



ach) (Fig. 9, top left panel). Nauplii are the most abundant prey in the pond, which is also reflected in simulated gut contents (Fig. 9). After day 20, the larger larval size opens up for a wider range of prey items and the importance of copepodites increases (Fig. 9).

#### Rules compared with random walk

Weight-at-age varied for larvae following different rules, and all rules perform better than a random movement strategy (Fig. 10a). Larvae moving according to rules HighP and HighG did best. The vertical movement during 32 days for a larva following rule HighG varies considerably over time (Fig. 10b). The frequent vertical repositioning is related to stomach dynamics: which habitat has maximum growth rates depends on stomach fullness, temperature, and prey abundance (Fig. 10c). The vertical position of the larva follows the depth where prey abundance satiates maximum growth at the highest possible temperature (Figs. 10c, 1a, and 1b). The average depth for the random walk converges towards an average of 2.5 m.

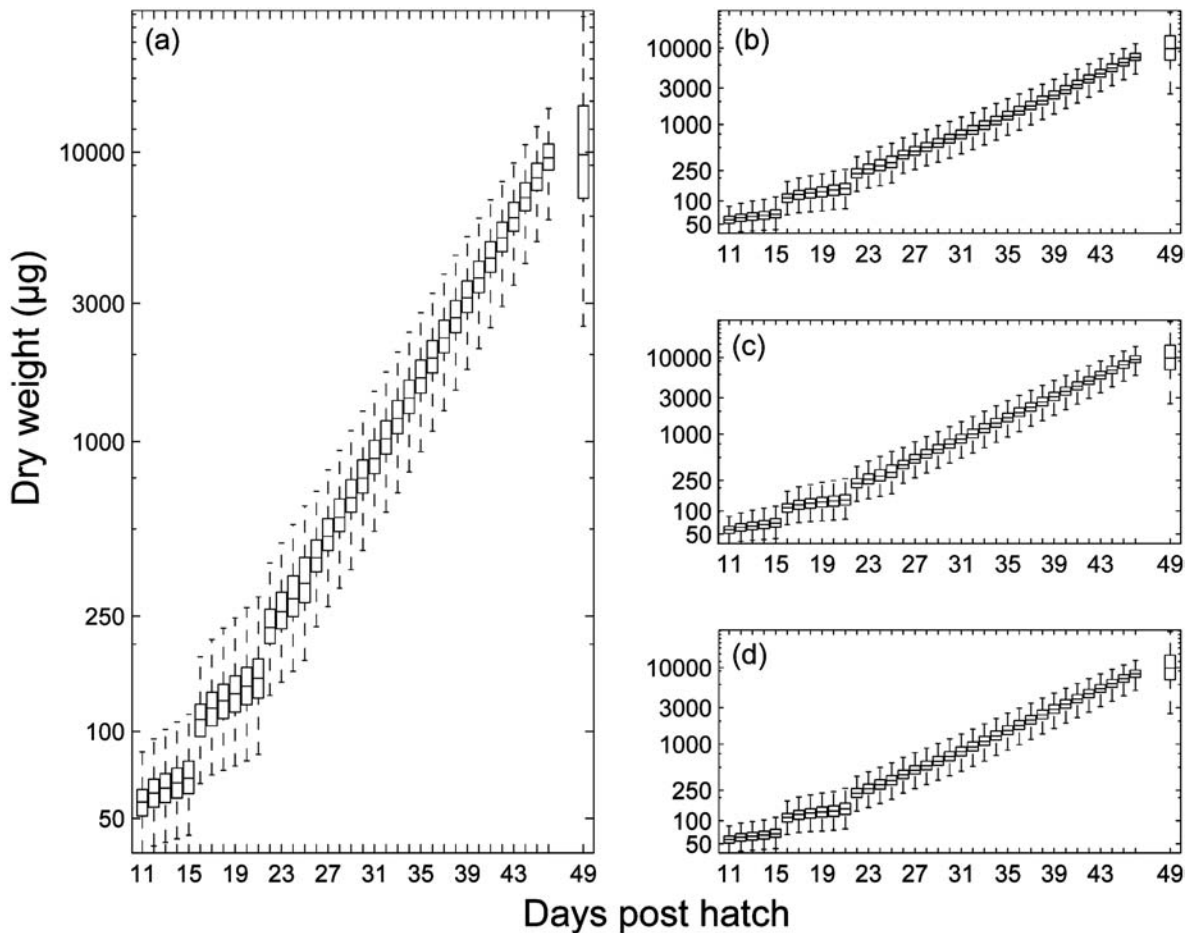
#### Discussion

Sensitivity analysis suggests that small changes in parameters or variables do not create large differences in simula-

tion results. This reassures us that the model is robust within the parameter space, possibly with the exception of the prey jump speed and the cod attack speed for small larva. The IBM uses the ratio between larva attack speed and prey escape speed (1/10), as discussed by Fiksen and MacKenzie (2002) in the calculation of the capture success. A larval attack speed of 10 standard lengths·s<sup>-1</sup> and a prey escape speed of 100 prey lengths·s<sup>-1</sup> are based on intermediate values from experiments (for details, see Fiksen and MacKenzie 2002). An increased ratio results in an increased capture success (restricted by the gape limitation of the larva) and vice versa. However, the selected ratio simulates a prey preference size of 5% of larval body length (Fiksen and MacKenzie 2002) and agrees well with observations by Munk (1997). This indicates that the chosen velocity values are sensible, although an improved version of this IBM would gain realism by including differences between prey species, e.g., contrast of prey to the background and difference in escape speed between species.

Smaller larvae are sensitive to changes in prey density, which is not surprising, as 2–4 nauplii·L<sup>-1</sup> seems to be the minimum values needed for larvae to sustain metabolism. Model results predict that larvae are able to grow at 2%–5%·day<sup>-1</sup> at quite low prey density (2 nauplii·L<sup>-1</sup>), although growth after 25 DPH at this prey density is severely limited.

**Fig. 8.** Simulated growth rates ( $\% \cdot \text{day}^{-1}$ ) for 160 individual larvae. Model runs are initialized with the observed (Folkvord et al. 1994) weight distribution at 11, 16, 22, and 26 days post hatch (DPH) (boxes) using four vertical positioning rules, (a) HighG (depth that yields the highest growth rate), (b) ObsD (depth where maximum abundances of larvae were observed during assessment), (c) HighT (depth of highest temperature), and (d) HighP (depth with highest prey biomass).



When we increased the prey density to  $10 \text{ nauplii} \cdot \text{L}^{-1}$ , the larvae achieved high growth rates for the first 25 DPH ( $500 \mu\text{g}$ ). As the body size of the larva reaches  $1000 \mu\text{g}$ , it seems that optimal growth is only viable to sustain if the diet includes copepodites.

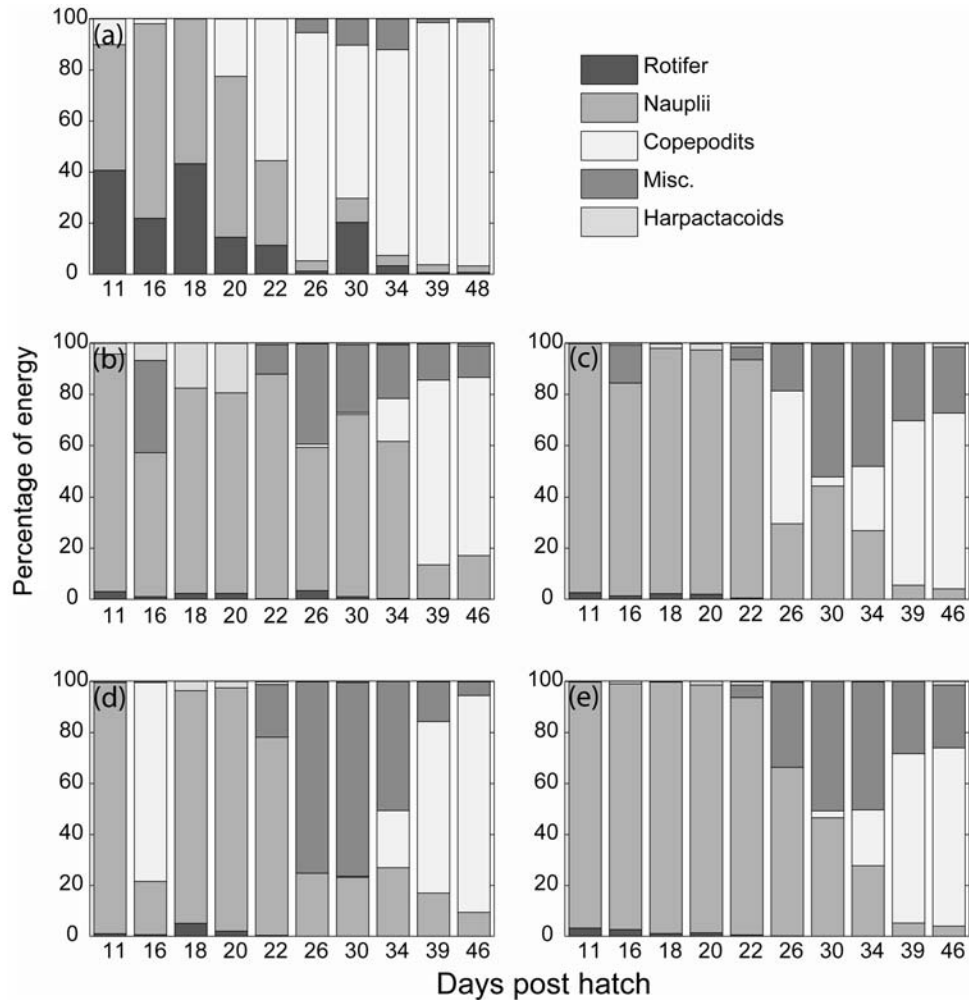
Light did not limit foraging in the pond, except for a short period at night (2200–0200), although food-limited growth through this period is avoided if the larva keeps a full stomach.

Early life history (growth and survival) of larval cod is determined from the larva's interaction with physical and biological properties, such as turbulence (Sundby et al. 1994; MacKenzie and Kiørboe 1995, 2000), light (Aksnes and Giske 1993; Aksnes and Utne 1997; Fiksen et al. 1998), temperature (Otterlei et al. 1999; Sundby 2000; Folkvord 2005), ocean transport (Werner et al. 1993; Vikebø et al. 2005), prey abundance (Cushing 1990; Beaugrand et al. 2003), and predators. Larval cod may be able to utilize its environment by adaptive vertical positioning. Model simulations indicate that active vertical behaviour in the pond does influence growth rates and is especially important for the first 5–25 DPH of feeding. This is not necessarily true in general but is of importance in our model setup where food

abundance is limited and spatially distributed. Simulations indicate a 2% difference in daily specific growth rate between rules for a pond of only 5 m depth. The simple rules may not be very applicable to natural conditions but indicate the potential gain of being flexible and actively seeking patches of prey to optimize its growth rate, particularly when stomach fullness is decreasing. We have used weight and growth rate as fitness a measure for comparison between rules. This was a natural choice, as mortality was not included in the model and the experimental habitat was predator free, although Folkvord et al. (1994) did observe an increased size-selective cannibalism as the experiment evolved. We are currently exploring the use of more sophisticated behavioural rules in situations with multiple trade-offs between growth, predation risk, drift trajectories, and dispersal (Fiksen et al., in press).

In natural environments, the larva has to consider the trade-off between foraging and risk from predators. In the nearly predator-free pond, Folkvord et al. (1994) observed that larvae aggregated along the bottom for the first week after release, before gradually dispersing throughout the water column. The dispersal corresponded to a period of low prey concentration and probably the end of yolk sac utilization.

**Fig. 9.** (a) Observed (Folkvord et al. 1994) and simulated energy content in the stomach according to choice of vertical positioning rule (b) ObsD (depth where maximum abundances of larvae were observed during assessment), (c) HighT (depth of highest temperature), (d) HighP (depth with highest prey biomass), and (e) HighG (depth that yields the highest growth rate). Prey categories are confined to rotifers, *Calanus finmarchicus* nauplii and copepodites, miscellaneous, and harpacticoids. The energetic contribution from these five prey categories was estimated using the conversion between prey weight and energy content from Blom et al. (1991).

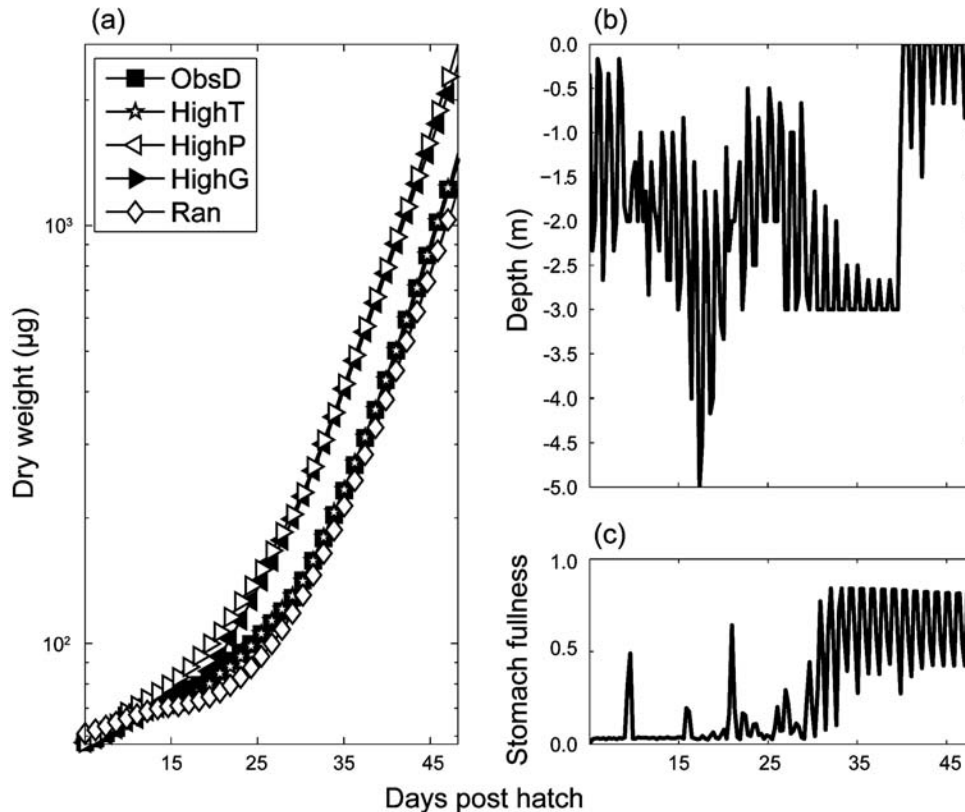


Larval cod that are able to maximize growth (HighG) avoid areas of low prey density. They also tend to find the depths where prey densities are able to sustain high growth rates at depths of high temperature. Small larvae are therefore able to grow fast, but their energy storage is low. It is also evident from the model results that even simple rules outperform random vertical behaviour. For the larvae to obtain growth rates comparable with what Folkvord et al. (1994) observed, it would therefore be tempting to say that the larvae would need some form of strategy. Information on to what extent larval cod are able to optimize the water column in this fashion and to migrate vertically is limited. Grønkvær and Wieland (1997) observed vertical distribution of small larvae (4–5 mm) in the Baltic Sea. The Baltic Sea is characterized by low-density surface water, making the eggs neutrally buoyant below the halocline (>45 m). Larval cod are visual feeders, and food and light at the depth of hatching are limited, causing the larvae to swim upward, closer to the surface, to forage. This behaviour is observed from the onset

of first feeding (2–5 DPH) and indicates the ability of small larvae to be able to adequately assess the environment. Larval behaviour is probably connected to environmental gradients, especially the gradient of light in a water column. Light is essential for detecting prey but also for larval exposure to predators. As the larvae grow in size, they develop a diel vertical migration pattern based on the trade-offs between feeding and the risk to predation (Lough and Potter 1993). Larval cod on Georges Bank, larger than 9 mm, seem to follow a diurnal cycle, moving into the surface layer (upper 20 m) at night and into deeper water (35 m) during the day (Lough and Potter 1993; Lough et al. 1996). This vertical behaviour is probably initiated when larvae reach 6–8 mm (Lough and Potter 1993).

Folkvord et al. (1994) observed that larvae fed mainly on rotifers and nauplii (80% of the stomach content) for the first 20 DPH and then switched to a diet of larger copepodites, contributing up to 90% of the energy and 20% of the prey number in the stomach at 48 DPH. Both simula-

**Fig. 10.** (a) Average simulated weight for 10 individuals that follow the rules ObsD (depth where maximum abundances of larvae were observed during assessment), HighT (depth of highest temperature), HighP (depth with highest prey biomass), and HighG (depth that yields the highest growth rate) compared with the average weight of 100 individuals that move randomly (Ran) and (b) depth position and (c) specific stomach content for a 32-day period of an individual that optimize the growth rate (HighG) (6 h running mean).



tions and observations indicate that nauplii are the main prey species for smaller larvae. A striking difference between observations and simulations is the high numbers of rotifers found in the gut analysis. This bias between observations and simulations could stem from underestimated sampling of rotifers, perhaps caused by patchy distribution of rotifers not captured by the sampling routines. Also, alternative prey such as ciliates may have been present in the pond but not detected in the sampling. Alternatively, the encounter rate with small prey is severely underestimated in the model, but it is difficult, then, to point out exactly which element of the feeding model is biased. Rotifers could also be detected at larger distance and encountered more frequently than anticipated owing to their movement pattern.

After day 20, the simulated larvae are able to capture and digest larger copepodites, but the level of copepodites in the stomach is lower in simulations compared with observations. Abundance of copepodites in the pond could have been higher than sampling data reveal, or perhaps larvae in the pond actively select larger prey.

The foraging model is biased towards the prey with the highest encounter rate, given that the size of the prey is feasible to capture for the larva. Larvae in natural conditions are often size selective and favour larger prey (McLaren and Avendano 1995; Munk 1995, 1997) if food is plentiful. Here, the mechanistic model merely includes passive selection resulting from the physical and biological characteris-

tics between the prey and the predator, some of which include functions of size.

An energy source for the larvae at the onset of exogenous feeding was phytoplankton. Dinoflagellates in combination with rotifers were observed by Theilacker and McMaster (1971) to provide anchovy larvae with enough energy to grow at a physiological optimal rate. Fossum and Ellertsen (1994) observed the dominance of phytoplankton in gut analysis of larval cod in Lofoten (Norway) for the first 2–3 days after the start of feeding. Folkvord et al. (1994) observed “green guts” in the stomach analysis, indicating active foraging on phytoplankton. This extra energy source could be vital for survival during the critical first days after hatching, as simulations with the observed zooplankton field were too low to provide the necessary amount of prey of the correct size range for the larvae to grow at a rate comparable with observations. It seems that the ability of larvae to utilize potential energy of, e.g., protozoans (von Herbing and Gallagher 2000) and phytoplankton (Pedersen et al. 1989; van der Meeren 1993; Lough and Mountain 1996), in food-limited areas may be crucial for first-feeding cod larvae.

Simulated and observed growth rates differ considerably for the first 17 days (22 DPH). One obvious error concerning this comparison is that the IBM does not account for size-dependent mortality. It is probable that size-dependent mortality removed the smallest individuals in the pond, especially regarding the low prey availability. The overall mortal-

ity to metamorphosis (12 mm) was very low (60%), but most effective during the first 2 weeks of the experiment (Folkvord et al. 1994). From the starvation control experiment, Folkvord et al. (1994) found that 90% of the total mortality occurred between day 15 and day 20. Differences between model results and observations are partly explained by the combination of an extra energy source in phytoplankton and size-dependent mortality. After 22 DPH, there is a strong resemblance to the model and experimental data, suggesting that the model is capable of simulating larval growth, given the correct input data.

In conclusion, the use of IBMs as tools for bringing knowledge and processes at an individual level to the population level is becoming increasingly popular (Grimm and Railsback 2005). IBMs as a reliable laboratory can help us understand how population patterns emerge from individual traits, how physical characteristics affect behavior of pelagic fish, and possibly the impact of climatic variability on individuals and populations. It is also a way to bridge experimental studies with modelling to generate understanding of patterns at a larger scale. However, to obtain reliable patterns, we need to develop IBMs that have been tested and used with data from natural conditions. Our model does not provide results with a perfect fit to observations but provides some hypotheses on the interaction between processes and the relative importance of processes. It also identifies where the model fails, although it is difficult to point exactly to particular processes. Possibly, the sampling procedure could also be the reason for some of the discrepancies. We also realize that there are likely to be substantial differences between natural environments and the macrocosm used here. This type of systematic use of IBMs can also give feedback to future experimental work.

Even in a pond of only 5 m depth, the light, prey, and temperature gradients are strong, and this research has pinpointed how larval vertical behaviour influence realized growth rates. Modelling efforts today often strive to explain both large- and small-scale processes combined by using coupled IBMs and three-dimensional physical models. The type of behaviour that the larvae exhibit in these model setups colours the simulated larval drift, distribution, and growth, and it is therefore important to consider implementing sound vertical behavior, e.g., as a function of larval condition (stomach fullness, larval size) and light (Fiksen et al., in press). The failure to do so could severely influence model results and conclusions.

## Acknowledgements

This work was financed by the Norwegian Research Council (project No. 155930/700) and is part of the ECOBE (NORWAY-GLOBEC) project. The authors thank J. Titelman for comments on early versions of the manuscript and K.A. Rose for help with the Latin Hypercube Sampling method.

## References

Aksnes, D.L., and Giske, J. 1993. A theoretical-model of aquatic visual feeding. *Ecol. Model.* **67**: 233–250.

- Aksnes, D.L., and Utne, A.C.W. 1997. A revised model of visual range in fish. *Sarsia*, **82**: 137–147.
- Bartell, S.M., Breck, J.E., Gardner, R.H., and Brenkert, A.L. 1986. Individual parameter perturbation and error analysis of fish bioenergetics models. *Can. J. Fish. Aquat. Sci.* **43**: 160–168.
- Beaugrand, G., Brander, K.M., Lindley, J.A., Souissi, S., and Reid, P.C. 2003. Plankton effect on cod recruitment in the North Sea. *Nature (London)*, **426**: 661–664.
- Blom, G., Otterå, H., Svåsand, T., Kristiansen, T.S., and Serigstad, B. 1991. The relationship between feeding conditions and production of cod fry (*Gadus morhua* L.) in a semi-enclosed marine ecosystem in western Norway, illustrated by use of a consumption model. *ICES Mar. Sci. Symp.* **192**: 176–189.
- Caparroy, P., Thygesen, U.H., and Visser, A.W. 2000. Modelling the attack success of planktonic predators: patterns and mechanisms of prey size selectivity. *J. Plankton Res.* **22**: 1871–1900.
- Cushing, D.H. 1990. Plankton production and year-class strength in fish populations — an update of the match/mismatch hypothesis. *Adv. Mar. Biol.* **26**: 249–293.
- Fiksen, Ø., and Folkvord, A. 1999. Modelling growth and ingestion processes in herring *Clupea harengus* larvae. *Mar. Ecol. Prog. Ser.* **184**: 273–289.
- Fiksen, Ø., and MacKenzie, B.R. 2002. Process-based models of feeding and prey selection in larval fish. *Mar. Ecol. Prog. Ser.* **243**: 151–164.
- Fiksen, Ø., Utne, A.C.W., Aksnes, D.L., Eiane, K., Helvik, J.V., and Sundby, S. 1998. Modelling the influence of light, turbulence and ontogeny on ingestion rates in larval cod and herring. *Fish. Oceanogr.* **7**: 355–363.
- Fiksen, Ø., Jørgensen, C., Kristiansen, T., Vikebø, F., and Huse, G. In press. Linking behavioural ecology and oceanography: larval behaviour determines growth, mortality, and dispersal. *Mar. Ecol. Prog. Ser.*
- Finn, N., Rønnestad, I., van der Meeren, T., and Fyhn, H.J. 2002. Fuel and metabolic scaling during the early life stages of Atlantic cod *Gadus morhua*. *Mar. Ecol. Prog. Ser.* **243**: 217–234.
- Folkvord, A. 2005. Comparison of size-at-age of larval Atlantic cod (*Gadus morhua*) from different populations based on size- and temperature-dependent growth models. *Can. J. Fish. Aquat. Sci.* **62**: 1037–1052.
- Folkvord, A., Øiestad, V., and Kvenseth, P.G. 1994. Growth-patterns of 3 cohorts of Atlantic cod larvae (*Gadus morhua* L.) studied in a macrocosm. *ICES J. Mar. Sci.* **51**: 325–336.
- Fossum, P., and Ellertsen, E. 1994. Gut content analysis of first-feeding cod larvae (*Gadus morhua* L.) sampled at Lofoten, Norway, 1979–1986. *ICES Mar. Sci. Symp.* **198**: 430–437.
- Gardner, R.H., and O'Neill, R.V. 1981. A comparison of sensitivity analysis and error analysis based on a stream ecosystem model. *Ecol. Model.* **12**: 173–190.
- Grimm, V., and Railsback, S.F. 2005. Individual based modeling and ecology. 1st ed. Princeton University Press, Princeton, N.J.
- Grønkjær, P., and Wieland, K. 1997. Ontogenetic and environmental effects on vertical distribution of cod larvae in the Bornholm Basin, Baltic Sea. *Mar. Ecol. Prog. Ser.* **154**: 91–105.
- Hinrichsen, H.-H., Möllmann, C., Voss, R., Köster, F.W., and Kornilovs, G. 2002. Biophysical modeling of larval Baltic cod (*Gadus morhua*) growth and survival. *Can. J. Fish. Aquat. Sci.* **59**: 1858–1873.
- Holling, C.S. 1966. The functional response of invertebrate predators to prey density. *Mem. Entomol. Soc. Can.* **48**: 1–86.
- Kjørboe, T. 1989. Growth in fish: are they particularly efficient? *Rapp. P.-v. Réun. Cons. Int. Explor. Mer.* **191**: 383–389.
- Letcher, B.H., Rice, J.A., Crowder, L.B., and Rose, K.A. 1996. Variability in survival of larval fish: disentangling components

- with a generalized individual-based model. *Can. J. Fish. Aquat. Sci.* **53**: 787–801.
- Lough, R.G., and Mountain, D.G. 1996. Effect of small-scale turbulence on feeding rates of larval cod and haddock in stratified water on Georges Bank. *Deep-Sea Res. Part II. Top. Stud. Oceanogr.* **43**: 1745–1772.
- Lough, R.G., and Potter, D.C. 1993. Vertical distribution patterns and diel migrations of larval and juvenile haddock *Melanogrammus aeglefinus* and Atlantic cod *Gadus morhua* on Georges Bank. *Fish. Bull.* **91**: 281–303.
- Lough, R.G., Caldarone, E.M., Rotunno, T.K., Broughton, E.A., Burns, B.R., and Buckley, L.J. 1996. Vertical distribution of cod and haddock eggs and larvae, feeding and condition in stratified and mixed waters on southern Georges Bank, May 1992. *Deep-Sea Res. Part II. Top. Stud. Oceanogr.* **43**: 1875–1904.
- Lough, R.G., Buckley, L.J., Werner, F.E., Quinlan, J.A., and Edwards, K.P. 2005. A general biophysical model of larval cod (*Gadus morhua*) growth applied to populations on Georges Bank. *Fish. Oceanogr.* **14**: 241–262.
- MacKenzie, B.R., and Kjørboe, T. 1995. Encounter rates and swimming behavior of pause–travel and cruise larval fish predators in calm and turbulent laboratory environments. *Limnol. Oceanogr.* **40**: 1278–1289.
- MacKenzie, B.R., and Kjørboe, T. 2000. Larval fish feeding and turbulence: a case for the downside. *Limnol. Oceanogr.* **45**: 1–10.
- MacKenzie, B.R., and Leggett, W.C. 1993. Wind-based models for estimating the dissipation rates of turbulent energy in aquatic environments — empirical comparisons. *Mar. Ecol. Prog. Ser.* **94**: 207–216.
- McLaren, I.A., and Avendano, P. 1995. Prey field and diet of larval cod on Western Bank, Scotian Shelf. *Can. J. Fish. Aquat. Sci.* **52**: 448–463.
- Megrey, B., and Hinckley, S. 2001. Effect of turbulence on feeding of larval fish: a sensitivity analysis using an individual-based model. *ICES J. Mar. Sci.* **58**: 1015–1029.
- Munk, P. 1995. Foraging behaviour of larval cod (*Gadus morhua*) influenced by prey density and hunger. *Mar. Biol.* **122**: 205–212.
- Munk, P. 1997. Prey size spectra and prey availability of larval and small juvenile cod. *J. Fish Biol.* **51**(Suppl. A): 340–351.
- Otterlei, E., Nyhammer, G., Folkvord, A., and Stefansson, S.O. 1999. Temperature- and size-dependent growth of larval and early juvenile Atlantic cod (*Gadus morhua*): a comparative study of Norwegian coastal cod and northeast Arctic cod. *Can. J. Fish. Aquat. Sci.* **56**: 2099–2111.
- Pedersen, T., Eliassen, J.E., Eilertsen, H.C., Tande, K.S., and Olsen, R.E. 1989. Feeding, growth, lipid composition, and survival of larval cod (*Gadus morhua* L.) in relation to environmental conditions in an enclosure at 70° in northern Norway. *Rapp. P.-v. Réun. Cons. Int. Explor. Mer.* **191**: 409–420.
- Rose, K.A. 1987. Sensitivity analysis in ecological simulation models. In *Systems and control encyclopedia: theory, technology, applications*. Edited by M.G. Singh. Oxford Press, Toronto, Ont. pp. 4230–4235.
- Rose, K.A., Brenkert, A.L., Cook, R.B., and Gardner, R.H. 1991a. Systematic comparison of ILWAS, MAGIC, and ETD watershed acidification models 2. Monte Carlo analysis under regional variability. *Water Resour. Res.* **27**: 2591–2603.
- Rose, K.A., Smith, E.P., Gardner, R.H., Brenkert, A.L., and Bartell, S.M. 1991b. Parameter sensitivities, Monte-Carlo filtering, and model forecasting under uncertainty. *J. Forecasting*, **10**: 117–133.
- Sundby, S. 2000. Recruitment of Atlantic cod stocks in relation to temperature and advection of copepod populations. *Sarsia*, **85**: 277–298.
- Sundby, S., Ellertsen, B., and Fossum, P. 1994. Encounter rates between first-feeding cod larvae and their prey during moderate to strong turbulent mixing. *ICES Mar. Sci. Symp.* **198**: 293–405.
- Theilacker, G.H., and McMaster, M.F. 1971. Mass culture of the rotifer *Brachionus plicatilis* and its evaluation as a food for larval anchovies. *Mar. Biol.* **10**: 183–188.
- van der Meeren, T. 1993. Feeding ecology, nutrition, and growth in young cod (*Gadus morhua* L.) larvae. *Dr. Sci.*, University of Bergen, Bergen, Norway.
- Vikebø, F., Sundby, S., Ådlandsvik, B., and Fiksen, Ø. 2005. The combined effect of transport and temperature on distribution and growth of larvae and pelagic juveniles of Arcto-Norwegian cod. *ICES J. Mar. Sci.* **62**: 1375–1386.
- von Herbing, I.H., and Gallager, S.M. 2000. Foraging behavior in early Atlantic cod larvae (*Gadus morhua*) feeding on a protozoan (*Balanion* sp.) and a copepod nauplius (*Pseudodiaptomus* sp.). *Mar. Biol.* **136**: 591–602.
- Werner, F.E., Page, F.H., Lynch, D.R., Loder, J.W., Lough, R.G., Perry, R.I., Greenberg, D.A., and Sinclair, M.M. 1993. Influences of mean advection and simple behavior on the distribution of cod and haddock early life stages on Georges Bank. *Fish. Oceanogr.* **2**: 43–64.
- Werner, F.E., MacKenzie, B.R., Perry, R.I., Lough, R.G., Naimie, C.E., Blanton, B.O., and Quinlan, J.A. 2001. Larval trophodynamics, turbulence, and drift on Georges Bank: a sensitivity analysis of cod and haddock. *Sci. Mar.* **65**: 99–115.